

C.J. Atkin<sup>o</sup> & D.I.A. Poll<sup>b</sup>

# Correlation Between Linear Stability Analysis and Crossflow Transition Near an Attachment Line

## Abstract

Results of exhaustive linear stability calculations are presented for the boundary layer flow near the attachment line of a yawed cylinder, the flow being that studied at length by Poll (1985). The results are represented following some dimensional analysis and demonstrate a clear transition onset position for all yaw angles and Reynolds numbers. Linear stability theory yields an unambiguous  $e^N$  correlation, in contrast to previous attempts to apply the method to crossflow instability.

## Introduction

The problem of transition on or near the leading edge of swept wings has been the subject of investigation for some years now. In addition to the problem of designing a laminar flow wing, where the leading edge is the most critical region, the phenomenon also impacts on the study of Reynolds number effects for wind-tunnel-to-flight extrapolation.

This particular investigation concerns crossflow transition close to a laminar attachment-line flow which derives initially from the instability associated with the inflectional nature of the velocity profiles in three-dimensional boundary layers. The principle of crossflow instability has been well documented since the work of Gregory *et al.* (1955) but the subsequent processes leading to transition are not universally understood, although progress has been made with respect to some specific mechanisms (see for example Bippes, 1991).

Prediction has proved a difficult exercise because the transition process is affected by a large number of parameters and it is not always clear exactly when and how these parameters should be taken into account. Current approaches to prediction vary from fully empirical criteria such as those discussed by Arnal *et al.* (1984) to direct numerical simulations (see Reed, 1994). The former methods attempt to generalise the transition phenomena and suffer from an insufficient treatment of the physics of the flow, while the latter, which investigate specific transition scenarios, are quite expensive and require extremely detailed information about the external flow and the initial disturbance environment. As such they are limited in scope for use in design. In between there are approaches which retain and discard varying amounts of physics such as the  $e^N$  approach

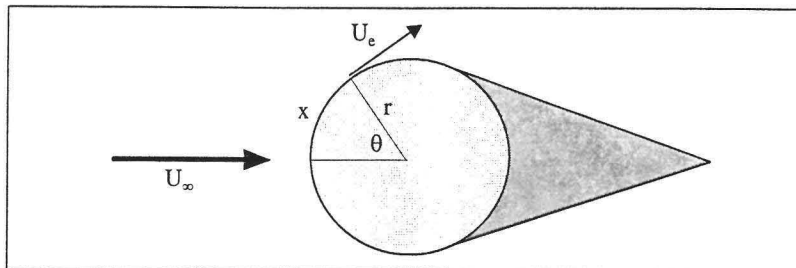


Figure 1: Cross-section of the yawed cylinder model.  $x$  is the distance along the surface,  $U_e$  the local velocity and  $U_\infty$  the free stream velocity all measured normal to the leading edge.

of Van Ingen (1956) and Smith & Gamberoni (1956) and the PSE method of Herbert (1991) and Bertolotti (1991).

The semi-empirical  $e^N$  method has been criticised in recent years because it often fails to yield a consistent  $N$ -factor correlation across a range of wind tunnel and flight test measurements, particularly for crossflow transition, and for its inability to account for receptivity or non-linear effects which are known to exist. However the method has been used with success to predict effects of suction and heat transfer on the growth of instabilities in the boundary layer, particularly when using a given wind tunnel. The method obviously works best when the position of transition is largely dictated by the exponential growth of small-amplitude disturbances.

More sophisticated methods yield more convincing results but for aerodynamic design simple  $e^N$  is already regarded as an expensive exercise and the modelling of receptivity and of non-linear effects may push the cost of transition analysis beyond the levels allowable for rapid design iterations. This is the motivation for persisting with the technique in the face of its mathematical limitations. The majority of effort on the  $e^N$  method is now concentrated on finding reliable correlations between wind tunnels and for extrapolating from wind tunnel to flight.

In this paper, which describes work performed late in 1993 at British Aerospace Regional Aircraft Ltd and at the Manchester School of Engineering, the authors present very consistent  $N$ -factor results for the flow over a yawed cylinder measured in different wind tunnels and using different models. The raw data have been in the literature for some time but the presentation and the stability analysis are new.

## Experimental arrangement

The flow being studied is that near the attachment line of an infinite-yawed cylinder (see Poll, 1985 for experimental details). A cross-section is shown in Fig. 1. The original data obtained at Cranfield were supplemented by tests performed

at the Goldstein Aeronautics Laboratory at Manchester University on a cylinder of twice the dimensions; the latter cylinder was laser-drilled for surface suction, although no suction results are presented here. In both sets of experiments the transition was set at given chordwise positions by varying the tunnel speed (and therefore local Reynolds number) for a particular angle of sweep. The variables in this problem therefore include model manufacture, surface finish, wind tunnel noise and tunnel turbulence intensity (up to 0.16%). These are all factors which are known to influence transition under various circumstances (see Bippes, 1991 and Saric, 1994).

The relevance of the yawed cylinder model to full-scale leading edges can be determined from dimensional analysis. In general the chordwise velocity distribution (see Fig. 1) for a lifting aerofoil can be expressed as a power series:

$$\frac{U_e}{U_\infty} = A \left( \frac{x}{l} \right) + B \left( \frac{x}{l} \right)^2 + C \left( \frac{x}{l} \right)^3 + \dots, \quad (1)$$

where  $l$ ,  $A$ ,  $B$  and  $C$  are constants. In the vicinity of the attachment line:

$$\frac{U_e}{U_\infty} \cong A \left( \frac{x}{l} \right) = \left( \frac{dU_e}{dx} \right)_{x=0} \frac{x}{U_\infty} = K \frac{x}{U_\infty}. \quad (2)$$

We now assume the leading edge flow to be infinite-swept, the free stream to be isentropic and homenthalpic, and the wall temperature to be constant at  $T_w$ . We restrict the analysis to flows without surface suction and concentrate on integral properties: that is, we do not consider wall-normal variations. Any property  $q$  of the boundary layer flow in the vicinity of the attachment line is thus a function of the following variables:

$$q = f(y, x, K, V_A, \rho_A, \mu_A, T_A, T_w, c_p, R), \quad (3)$$

where  $V$  is the spanwise velocity,  $R$  the gas constant and the subscript  $A$  refers to conditions at the attachment line. We neglect surface finish, tunnel turbulence and tunnel noise in the analysis. From Buckingham's II theorem, nine independent variables and four dimensions (mass, length, time and temperature) yield five dimensionless groups. We choose:

$$\sqrt{\frac{V_A^2}{\nu_A K}} = \bar{R}, \quad \left( \frac{x^2 K}{\nu_A} \right) = \frac{U_e x}{\nu_A} = R_x, \quad M_A, \quad \gamma \quad \text{and} \quad \frac{T_w}{T_A}. \quad (4)$$

By limiting our consideration to air and to adiabatic flow, we conclude that any dimensionless property  $Q$  of the boundary layer flow is governed by the parameters:

$$Q = f(\bar{R}, R_x, M_A). \quad (5)$$

This tells us that the wing sweep is not *explicitly* a parameter in the problem. In terms of compressibility, the relevant Mach number is the *spanwise* Mach number

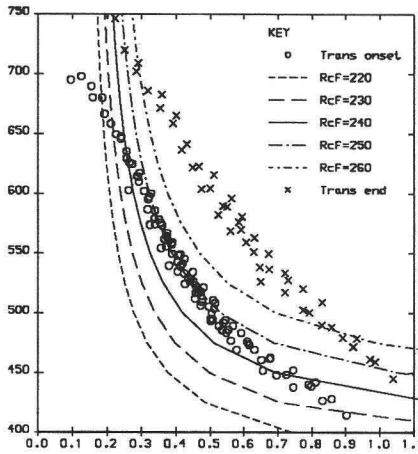


Figure 2: Transition onset and completion for a yawed cylinder plotted with curves of constant crossflow Reynolds number.

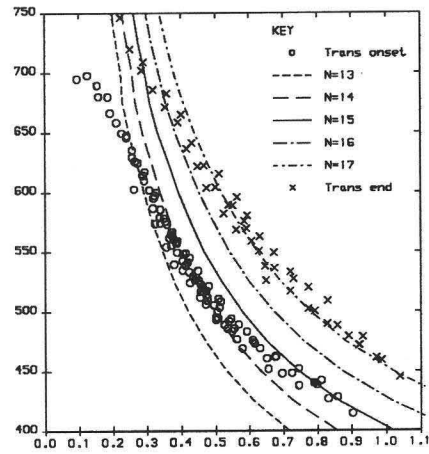


Figure 3: Transition onset and completion plotted with  $N$ -factor curves calculated for a cylinder yawed at  $30^\circ$ , using integration strategy 1.

which, for all current transport wing applications, is in the low subsonic regime. To a good approximation, then, the flow near the attachment line depends on  $\bar{R}$  and  $R_x$  alone, whether on a low speed cylinder model or a transport aircraft leading edge. The cylinder model can thus provide data directly relevant to the full scale aircraft.

The power of the dimensional analysis is demonstrated by re-plotting the results of Poll (1985) and adding the more recent data collected at Manchester in Fig. 2. The data generally cover values of  $\bar{R}$  above those currently encountered on transport aircraft ( $\bar{R} > 400$ ) and extend into the region where one finds attachment line instability,  $\bar{R} > 581$ . Work is in progress at the present time to extend the range of data to lower values of  $\bar{R}$  and higher values of  $R_x$ . The impressive collapse justifies the neglect of surface finish and tunnel turbulence and noise levels in the above dimensional analysis. However Bippes (1991) and Saric (1994) both find that transition dominated by stationary crossflow vortices is strongly dependent on these parameters, which suggests that transition in these experiments is determined not by the stationary modes but by some other mechanism. Whether this is due to the magnitude of the tunnel turbulence or whether this is a feature of transition in strongly accelerating flow remains to be established.

The advantages of this collapse is that the yawed cylinder flow is expressed as a two-parameter problem where both parameters have been fully explored. The results are then a useful benchmark for empirical transition prediction methods, such as the crossflow Reynolds number  $R_{cf}$  which is also plotted on Fig. 2.  $R_{cf}$  is defined here as  $w_{max} y_{10\%} / \nu_e$  where  $w$  is the crossflow velocity within

the boundary layer and  $y_{10\%}$  is the height at which  $w$  drops to one-tenth of its maximum value  $w_{max}$ . The correlation between  $R_{cf}$  and the experimental results is good only between  $500 \leq \bar{R} \leq 600$ .

### Boundary layer and stability analysis

The cylinder boundary layer flow was calculated for various yaw angles, assuming that the chordwise velocity distribution was that given by potential flow:

$$\frac{U_e}{U_\infty} = 2 \sin \theta = 2 \frac{x}{r} \frac{\sin \theta}{\theta}, \quad (6)$$

if  $\theta$  is small:

$$\frac{U_e}{U_\infty} \cong 2 \frac{x}{r}, \quad (7)$$

which represents swept Hiemenz flow. This has an analytical solution (see Rosenhead, 1963) and these analytical profiles were also used for stability calculations. The cylinder experiment was used to evaluate the 'black box' operation of a linear stability method developed at British Aerospace Regional Aircraft Ltd and validated during the European Laminar Flow Investigation programme (ELFIN). The code employs the spatial formulation described by Mack (1984) and the compact-difference scheme of Malik (1988). The method also accounts for the curvature terms arising from the use of body- and streamline-conforming co-ordinates (see for example de Bruin, 1990). Aside from the modelling deficiencies already described, linear stability theory also suffers from the need to know the frequency  $\omega$ , spatial wavenumber  $k$  and the phase speed direction  $\varphi$  of an unstable wave in the boundary layer *before* being able to calculate the amplification rate  $\alpha_i$ . However for flows which are often revisited, such as aerofoil flows at subsonic and transonic speeds, one can find empirical relations expressing  $k$  and  $\omega$  as functions of  $R_x$  and  $\varphi$ . These are sufficiently reliable to allow automated stability calculations without the need for manual input of frequencies or other wave properties: this approach was proven during the calculation of the cylinder  $N$ -factors for the full range of  $\bar{R}$  and  $R_x$ . In three-dimensions one must find all the amplified modes within the boundary layer for each combination of  $R_x$ ,  $\varphi$  and  $\omega$ . The amplification rates are then integrated with respect to  $x$  (and therefore  $R_x$ ) subject to certain constraints on  $\omega$  and  $\varphi$ : the frequency of each disturbance is invariant, but having assumed locally parallel mean flow, one must further assume a relation  $f(\varphi) = \text{constant}$  to determine how the physical properties of the wave vary with  $R_x$ : this is the ray tracing or 'integration strategy' problem. Some workers take  $\varphi$  to be constant, but Mack (1983) suggested that, for infinity-yawed flows, the spanwise wavenumber (SWN) should be constant:

$$f(\varphi) = k \sin(\varphi + \phi) = k_z, \quad (8)$$

where  $\phi$  is the angle between the local streamline and the  $x$  vector normal to the leading edge. This approach yields  $m \times n$  integrations as follows:

$$N_{a,b} = \int_{\alpha_i=0}^{R_{x'}=R_x} \alpha_i(x', \omega = \omega_a, f(\varphi) = k_{z,b}) dx' \quad \text{for } a = 1, \dots, m \quad (9)$$

$$b = 1, \dots, n$$

One must ensure that the 'worst' case (largest  $N$ -factor) is included in the analysis; fortunately it is quite simple to determine an appropriate range of  $k_z$  values at an early stage in the calculations. Arnal (1984) and others have used the 'envelope' strategy, which involves maximising  $\alpha_i(\varphi)$  at each boundary layer station  $R_x$  such that:

$$(\partial \alpha_i / \partial \varphi) |_{\omega} = 0. \quad (10)$$

This approach reduces the number of  $N$ -factor curves to  $m$ :

$$N_a = \int_{\alpha_i=0}^{R_{x'}=R_x} \alpha_{i, \max}(x', \omega = \omega_a) dx' \quad \text{for } a = 1, \dots, m. \quad (11)$$

Maximising  $\alpha_i(\varphi)$  may be marginally less expensive than the 'shotgun' approach required for the SWN strategy, but there is a risk that it converges only to a local rather than an absolute maximum in the  $\alpha_i$  vs.  $\varphi$  curve: hence it can be ambiguous.

An envelope of most-amplified modes  $N_{\max} = f(R_x)$  is compiled from the  $m \times n$  or  $m$  integrations and the analysis is repeated for different  $\bar{R}$  to obtain  $N_{\max} = f(\bar{R}, R_x)$ . Selected curves of constant  $N_{\max}$  can then be plotted against the experimental data. For each boundary layer calculation in this investigation eigenvalues were obtained over a range of 17  $R_x$  stations, 10 frequencies and 20 values of  $k_z$ . Total CPU time for 15 values of  $\bar{R}$  was 45 minutes on an 8-bit Silicon Graphics Indy 4600 workstation running at 100 MHz.

## Results

Fig. 3 shows the stability results for the cylinder at 30° sweep using the SWN strategy. The correlation is significantly better than that with  $R_{cf}$  (Fig. 2) particularly at lower values of  $\bar{R}$  where the curves are tangential to the experimental results. Transition onset corresponds to  $N = 14 \pm 1$  for the range  $400 \leq \bar{R} \leq 650$ , above which one encounters attachment line instabilities which would affect the experimental results but which are not modelled in the stability analysis. Fig. 4 confirms that the results are practically identical when the analysis is performed on swept Hiemenz flow except for large  $R_x$ , small  $\bar{R}$ : this is the region where the approximation  $\sin \theta \cong \theta$  implicit in equation (7) is invalid. These differences are magnified at larger sweep angles.

Fig. 5 shows how the envelope strategy improves the fit, giving a different  $N$  value of about 18 for most of the  $\bar{R}$  range. Integrating with constant  $\varphi$  yields a slightly worse fit than the two examples shown, particularly at lower values of

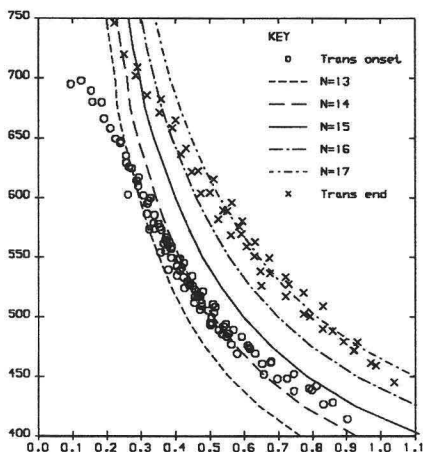


Figure 4: Transition positions and  $N$ -factor curves (SWN strategy) for swept Hiemenz flow.

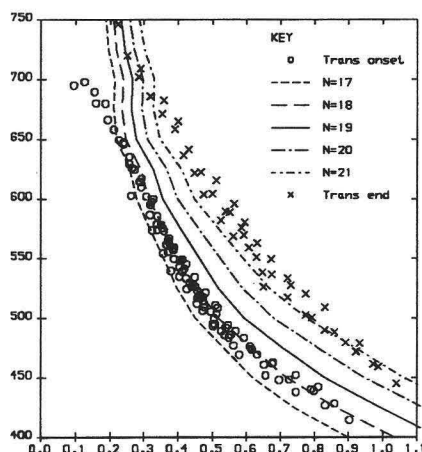


Figure 5: Transition positions and  $N$ -factor curves (**envelope strategy**) for a cylinder yawed at  $30^\circ$ .

$\bar{R}$ , giving  $15 \leq N \leq 18$ , but all three methods would probably satisfy engineering requirements for this particular set of data.

Fig. 6 shows the effect of surface and streamline curvature treatment for the SWN strategy. The quality of the  $N$ -factor correlation does improve markedly below  $\bar{R}=600$  to give a very narrow band around  $N=15$ . Surface curvature improves the fit while streamline curvature increases  $N$ . For the envelope strategy curvature increases  $N$  to about 18.5, but the fit is slightly poorer. Finally, Fig. 7 shows the detrimental effect of considering only stationary modes. This result is unaffected by either integration strategy or curvature effects.

## Conclusions

Dimensional analysis of the flow near a swept attachment line has shown that transition position is a function of  $\bar{R}$  and  $R_x$ . The variations in surface finish and wind tunnel environment during the experiments have not had a discernible effect on the results. The results of the linear stability analysis generally correlate well with the experimentally measured transition onset positions. The correlation is a significant improvement on that obtained with the crossflow Reynolds number. Best results are obtained from the envelope integration strategy and from the spanwise wavenumber strategy with curvature terms included. The latter strategy has a better physical basis for infinite-swept flows. Including curvature terms in the analysis alters the value of the  $N$ -factor for both integration strategies, but only improves the correlation for the SWN strategy.

The experimental observations (Poll, 1985) reveal the presence of both stationary and travelling disturbances ahead of the transition region. The linear

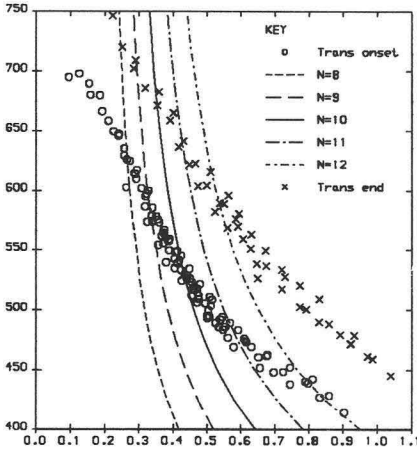


Figure 6: Transition positions and  $N$ -factor curves (SWN strategy) for a cylinder yawed at  $30^\circ$  including surface and streamline curvature effects.

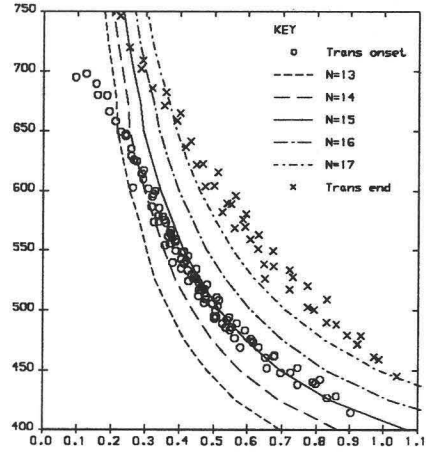


Figure 7: Transition positions and stationary mode  $N$ -factors (SWN strategy) for a cylinder yawed at  $30^\circ$ .

stability analysis, however, only correlates well when travelling modes are considered, prompting one of two conclusions: that in this flow there is a significant region of linear-theory-type wave growth, the travelling modes proving dominant over the stationary modes; or that the results presented here are a fantastic coincidence, given that linear stability analysis may be totally inapplicable to this problem. The dominance of stationary modes is usually associated with higher free-stream turbulence levels, but it is not clear how the presence of a strong, uniform chordwise velocity gradient influences the transition behaviour.

The values of  $N$ -factor from the SWN strategy are believed to be higher than those previously recorded for any type of disturbance in a wind tunnel. The work of Malik *et al.* (1994) suggests that non-parallel effects would be small. This does not invalidate the use of the  $e^N$  method as an engineering tool, but confirms that there are different flow fields requiring different values of  $N$ . Neither does the quality of the  $N$ -factor correlation imply that the transition process is wholly linear: simply that here the non-linear growth is either short in extent or can be represented by an extension of the linear growth regime. Future work will extend the experimental database to flows with suction and to situations where  $\bar{R}_x < 400$  and/or  $R_x > 1$  million.

## Acknowledgements

The authors would like to acknowledge the support of British Aerospace Regional Aircraft Ltd, Manchester University School of Engineering, and the UK Department of Trade and Industry.

## References

- Arnal, D., Coustols, E. & Juillen, J.C. 1984 – Experimental and theoretical study of transition phenomena on an infinite swept wing. *La Recherche Aérospatiale* **1984-4**.
- Arnal, D. 1984 – Boundary layer transition: predictions based on linear theory. *AGARD report R-793*, 2-1.
- Bertolotti, F.P. 1991 – Linear and non-linear stability of boundary layers with streamwise varying properties. *Ph.D. Thesis, Ohio State University, Columbus, Ohio*.
- Bippes, H. 1991 – Experiments on transition in three-dimensional accelerated boundary layer flows. *Proc. R.Ae.S. Conf. Boundary Layer Transition and Control*, Cambridge.
- De Bruin, A.C. 1990 – Linear boundary layer stability theory in orthogonal curvilinear co-ordinates. *NLR TR 90385 L*.
- Gregory, N., Stuart, J. T. & Walker, W. S. 1955 – On the stability of three-dimensional boundary layers with applications to the flow due to a rotating disk. *Phil. Trans. Roy. Soc. Lond. A* **248**, 155-199.
- Herbert, Th. 1991 – Boundary layer transition – analysis and prediction revisited. *AIAA paper 91-0737*.
- Mack, L.M. 1984 – Boundary layer stability theory. *AGARD report R-709*, paper no. 3.
- Malik, M.R. 1988 – Numerical methods for hypersonic boundary layer stability. *High Technology Corporation Report 88-6*.
- Malik, M.R., Li, F. & Chang, C.L. 1994 – Crossflow disturbances in three-dimensional boundary layers: non-linear development, wave interaction and secondary instability. *J. Fluid Mech.* **268**, 1-36.
- Poll, D.I.A. 1985 – Some observations of the transition process on the windward face of a long yawed cylinder. *J. Fluid Mech.* **150**, 329-356.
- Reed, H.L. 1984 – Direct numerical simulation of transition: the spatial approach. *AGARD report R-793*, paper no. 5.
- Rosenhead, L. 1963 – Laminar boundary layers. *Oxford University Press*, pp. 232 & 471.
- Saric, W.S. 1984 – Physical description of boundary layer transition: experimental evidence. *AGARD report R-793*, paper no. 1.
- Smith, A.M.O. & Gamberoni, N. 1956 – Transition, pressure gradient and stability theory. *Douglas Aircraft Company Report ES 26388*.
- Van Ingen, J.L. 1956 – A suggested semi-empirical method for the calculation of the boundary layer transition region. *Delft University of Technology, Dept. of Aero. Eng., Report no VTH-74*.

**Authors' addresses**

<sup>o</sup>Defence Research Agency  
Farnborough  
Hants, GU14 6TD  
United Kingdom

<sup>p</sup>College of Aeronautics  
Cranfield University  
Beds, MK41 XXX  
United Kingdom